This is the accepted manuscript of an article published as:
Noncovalent Interactions in Peri-Substituted Chalconium Acenaphthene and Naphthalene Salts: A Combined Experimental, Crystallographic, Computational, and Solid-State NMR Study
Knight, F. R., Randall, R. A. M., Arachchige, K. S. A., Wakefield, L., Griffin, J. M., Ashbrook, S. E., Buehl, M., Slawin, A. M. Z. & Woollins, J. D. 15 Oct 2012 In : Inorganic Chemistry. 51, 20, p. 11087-11097

Non-covalent interactions in *peri*-substituted chalconium acenaphthene and naphthalene salts; a combined experimental, crystallographic, computational and solid state NMR study

Fergus R. Knight,* Rebecca A. M. Randall, Kasun S. Athukorala Arachchige, Lucy Wakefield, John M. Griffin, Sharon E. Ashbrook, Michael Bühl, Alexandra M. Z. Slawin, J. Derek Woollins.

EaStCHEM School of Chemistry, University of St Andrews, St Andrews, Fife, KY16 9ST, U.K.; E-mail: frk@st-andrews.ac.uk; Fax: (+44) 1334 463384; Tel: (+44)1334 463829.

KEYWORDS X-ray structure, Solid State NMR, DFT, non-covalent, 3c-4e, hypervalency, intramolecular, chalconium salt, peri-substitution, acenaphthene, naphthalene.

Supporting Information Placeholder

ABSTRACT: Twelve related monocation chalconium salts [{Nap(EPh)(E` Ph)Me}$^{+}${$CF_3SO_3$}] **2-4**, [{Acenap(Br)(EPh)Me}{$CF_3SO^3$}] **5-7** and [{Acenap(EPh)(E` Ph)Me}$^{+}${CF_3SO_3}] **8-13**, have been prepared and structurally characterized. For their synthesis naphthalene compounds [Nap(EPh)(E` Ph)] (Nap = naphthalene-1,8-diyl; E/E` = S, Se, Te) **N2-N4** and associated acenaphthene derivatives [Acenap(EPh)(E` Ph)] (Acenap = acenaphthene-5,6-diyl; E/E` = S, Se, Te) **A5-A13** were independently treated with a single molar equivalent of methyl trifluoromethanesulfonate [MeOTf]. In addition, reaction of bis-tellurium compound **A10** with two equivalents of MeOTf afforded the doubly methylated dication salt [{Acenap$(TePhMe)_2$}$^{2+}${$(CF_3SO_3)_2$}$^{2-}$}] **14**. Distortion of the rigid naphthalene and acenaphthene backbone away from the ideal was investigated in each case and correlated in general with the steric bulk of the interacting atoms located at the proximal *peri*-positions. Naturally, introduction of the ethane linker in acenaphthene compounds increased the splay of the bay region compared with equivalent naphthalene derivatives resulting in greater *peri*-distances. The conformation of the aromatic rings and subsequent location of p-type lone-pairs has a significant impact on the geometry of the *peri*-region, with anomalies in *peri*-separations correlated to the ability of the frontier orbitals to take part in attractive or repulsive interactions. In all but one of the monocations a *quasi*-linear three-body C_{Me}-E···Z (E = Te, Se, S; Z = Br/E) fragment provides an attractive component for the E···Z interaction. Density-functional studies have confirmed these interactions and suggested the onset of formation of three-center, four-electron bonding under appropriate geometric conditions, becoming more prevalent as heavier congeners are introduced along the series. The increasingly large *J* values for Se-Se, Te-Se and Te-Te coupling observed in the ^{77}Se and ^{125}Te NMR spectra for **1**, **3**, **4**, **9**, **10** and **13** give further evidence for the existence of a weakly-attractive through-space interaction.

INTRODUCTION

Understanding the nature of atomic interactions and the strength of chemical bonds is an integral feature underpinning all aspects of chemistry, biology and materials science and as such has always attracted great attention. Pioneering work on the electronic theory of the covalent bond led to a greater understanding of strong bonding (covalent/ionic),[1] but ambiguity over the role of weak inter- and intra-molecular non-covalent interactions continues to intrigue chemists.[2-4] Designing structural architectures which invoke novel and unusual bonding interactions is indispensable for developing the theory of non-bonded forces and the chemical bond and is therefore an intriguing field of study.[5,6]

Non-covalent interactions can be attractive or repulsive in nature and are continually being highlighted within a diverse range of research fields,[2,3,7] with implications in drug design, supramolecular chemistry, materials and nanoscience.[8,9] The advance in X-ray crystallography exposed the importance of non-bonded forces with respect to thermodynamic stability, molecular geometry, self-assembly, crystal packing, reactivity and biological activity,[2,3,7-9] with a wide variety of forces emerging in the process (hydrogen bonding, ion-ion interactions, van der Waals forces, ion-dipole interactions, π-π stacking, dipole-dipole interactions).[3,7] Whilst Hydrogen bonding (NH···O, OH···O) is the most dominant type of non-covalent interaction,[7,10] less common CH···O[7,11] and CH···π[7,12] interactions (non-conventional hydrogen bonding) and short van der Waals forces between halogen and chalcogen congeners have recently emerged.[3,7,13]

In this context, rigid organic backbones that are able to constrain bulky halogen and chalcogen congeners in sterically demanding positions, at distances closer than the sum of their

respective van der Waals radii, provide ideal systems with which to study these weak non-bonded interactions.[5,6] Such bonding situations can be accomplished by a double substitution of the heavier congeners of Groups 16 and 17 at the *peri*-positions of naphthalene (positions 1 and 8)[14] and related 1,2-dihydroacenaphthylene (acenaphthene; positions 5 and 6).[15] The close proximity of the *peri*-atoms induces a direct overlap of orbitals leading to the onset of weakly-bonding interactions.[6] Electrostatic repulsion due to steric crowding forces the usually rigid naphthalene/acenaphthene carbon framework to distort, thus relaxing the geometry of the backbone.[16-18] Nevertheless, a distinguishing feature of *peri*-substitution is the ability to relieve steric strain via attractive intramolecular interactions operating between *peri*-substituents and ultimately acquiring a relaxed geometry by forming a direct bond between the *peri*-atoms.[6,16,19] The balance between, attractive and repulsive forces, bonding and non-bonding, occurring in the *peri*-region and within sub-van der Waals distances, gives these organic backbones their unique reactivity, structure and bonding.[6,14-18]

We have previously utilized the unique geometric constraints associated with *peri*-substitution and the rigidity of the naphthalene and acenaphthene backbones to investigate non-covalent forces occurring in mixed-donor ligands. Our early work focused on naphthalene, synthesizing dichalcogenide ligands[20] and unusual phosphorus compounds[21] and more recently mixed-donor phosphorus-chalcogen systems.[22] In the course of our investigation of non-bonding interactions we prepared a series of 1,8-disubstituted naphthalene derivatives that contain chalcogen atoms occupying the *peri*-positions [{Nap(EPh)(E` Ph)} (E = S, Se, Te)][23,24] and a similar mixed halogen-chalcogen series [{Nap(X)(EPh)} (X = Br, I; E = S, Se, Te)].[25,26] In a continuation of our work we have employed the alternative acenaphthene scaffold to prepare an analogous series of halogen-chalcogen [{Acenap(EPh)(E` Ph)} (E = S, Se, Te)] and chalcogen-chalcogen [{Acenap(EPh)(E` Ph)} (E = S, Se, Te)] systems.[27,28]

As might be expected, compounds accommodating heavier congeners in the proximal *peri*-positions, generally exhibit greater steric strain leading to increased molecular distortion of the rigid organic framework and subsequently greater *peri*-separations.[23,25,27] Naturally, acenaphthene derivatives display a greater distortion compared with analogous naphthalene compounds but the two series follow a similar trend.[27] Whilst the size of the *peri*-atoms has a significant impact on the degree of steric congestion and subsequent molecular distortion, the conformation of the aromatic ring systems and subsequent location of p-type lone-pairs dominates the geometry of the *peri*-region.[27] Differences in *peri*-separations observed for compounds adopting differing conformations of the *peri*-substituted phenyl group can be correlated to the ability of the frontier orbitals of the halogen or chalcogen atoms to take part in attractive or repulsive interactions. When the axis of the chalcogen p-orbitals aligns along the mean aromatic plane (A or AA type conformations, see below for definitions) repulsion is relatively high.[6,27,29] Conversely, a parallel alignment of the chalcogen p-orbitals to the mean plane (B or AB type conformations) reduces the repulsive interactions and notably shorter *peri*-separations with respect to the size of the atoms are observed.[6,27,29] Additionally, the B/AB type configuration affords a quasi-linear three-body fragment across the *peri*-gap, which appears to promote the formation of an attractive three-center, four electron type interaction.[27]

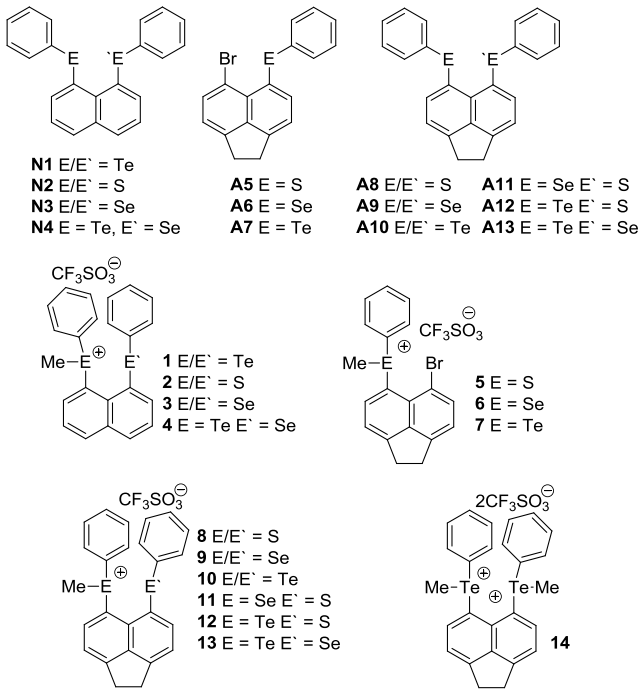

Figure 1. Monocation (1-13) and dication (14) chalconium salts formed from the reaction of naphthalene N1-N4 and acenaphthene A5-A13 derivatives with methyl trifluoromethanesulfonate (methyl triflate).

Evidence supporting a weak non-covalent *peri*-interaction in AB type compounds Nap(TePh)(SePh) **N4** and Acenap(TePh)(SePh) **A13** (Figure 1) is observed in their respective ^{125}Te NMR spectra.[23,27] The proton-decoupled ^{125}Te NMR spectrum of **N4** in $CDCl_3$ exhibits a single peak at δ = 687.6 ppm with clearly resolved satellite peaks due to ^{125}Te-^{77}Se coupling, with a large coupling constant of J_{TeSe} 834.0 Hz and similarly for **A13**, δ_{Te} = 663.4 ppm, J_{TeSe} 715.6 Hz.[23,27]

Furukawa *et al.* identified a similar interaction between telluronio-tellurenyl groups at the *peri*-positions of telluronium salt **1** (Figure 1) formed following treatment of 1,8-bis(phenyltelluro)naphthalene [Nap(TePh)$_2$] **N1** (Figure 1) with methyl trifluoromethanesulfonate (methyl triflate).[30] The ^{125}Te NMR spectrum of **1** showed two peaks at δ = 656 ppm (Te$^+$) and δ = 557 ppm (Te), each peak exhibiting satellites due to ^{125}Te-^{125}Te coupling and the large coupling constants of J_{TeTe} = 1093 Hz, attributed to a *peri*-interaction.[30]

The work presented here complements our earlier studies of non-covalent interactions in naphthalene and acenaphthene chalcogenides[23,25,27] and the work initially undertaken by Furukawa *et al.* on tellurium-tellurium *peri*-interactions in 1,8-ditelluronaphthalenes.[30] Herein we report a complete synthetic and structural study of associated monocation chalconium salts **2-13** and dication **14** formed from the reaction of naphthalenes **N2-N4**[23] and acenaphthenes **A5-A13**[27] with methyl triflate and an investigation of the potential non-bonding interactions associated with these types of systems (Figure 1).

Table 1. ^{77}Se and ^{125}Te NMR Spectroscopy Data[a]

	N3[23]	**3**	**A6**[27]	**6**	**A9**[27]	**9**	**A11**[27]	**11**		**N4**[23]	**4**	**A13**[27]	**13**
peri-atoms	Se, Se	Se^+, Se	Se, Br	Se^+, Br	Se, Se	Se^+, Se	Se, S	Se^+, S		Te, Se	Te^+, Se	Te, Se	Te^+, Se
^{77}Se solution NMR	428.6	435.9, 391.8	423.7	420.4	408.3	422.3, 365.7	433.7	430.7		362.8	346.9	340.7	322.6
^{77}Se solid-state NMR	-	-	-	-	426.1, 400.0	427.0, 375.4	432.8	441.8	-	-	-	350.0	335.9, 319.2
J (solution NMR)	-	166.9	-	-	-	140.7	-	-	-	-	428.9	-	381.5
	N1[23]	**1** Error! Bookmark not defined.	**A7**[27]	**7**	**A10**[27]	**10**	**A12**[27]	**12**	**14**				
peri-atoms	Te, Te	Te^+, Te	Te, Br	Te^+, Br	Te, Te	Te^+, Te	Te, S	Te^+, S	Te^+, Te^+				
^{125}Te solution NMR	620.2	656.0, 557.0	696.0	693.2	585.9	641.1, 521.6	689.4	693.9	677.0	687.6	705.7	663.4	679.2
J (^{125}Te solution NMR)	-	1093.0	-	-	-	945.8	-	-	-	-834.0	428.9	-715.6	381.5
^{125}Te solid-state NMR	-	-	-	-	595.2, 523.1	665.4, 551.1	704.6	695.2	-	-	-	684.0	705.8, 682.1

[a] Solution spectra of parent compounds, **3** and **4** were run in $CDCl_3$, spectra of acenaphthene chalconium salts were run in CD_3CN; δ (ppm), *J* (Hz).

RESULTS AND DISCUSSION

Naphthalene compounds [Nap(EPh)(E`Ph)] (Nap = naphthalene-1,8-diyl; E/E` = S, Se, Te) **N2**-**N4**[23] (Figure 1) and associated acenaphthene derivatives [Acenap(EPh)(E`Ph)] (Acenap = acenaphthene-5,6-diyl; E/E` = S, Se, Te) **A5**-**A13**[27] (Figure 1), were independently treated with methyl trifluoromethanesulfonate [MeOTf]. For the synthesis of monocation chalconium salts **2**-**13** (Figure 1), methylation reactions were carried out using a 1:1 molar ratio of MeOTf to chalcogen derivative and run in dichloromethane under an oxygen- and moisture-free nitrogen atmosphere [yield: 87-96%].

Under identical reaction conditions, treatment of 5,6-bis(phenyltelluro)acenaphthene **A10**[27] with two molar equivalents of MeOTf afforded the dication chalconium salt **14** (yield 54%). Corresponding reactions of the remaining group of chalcogen derivatives with a similar loading of methyl triflate exclusively afforded the monocation chalconium salt in each case. All the compounds obtained (**2**-**14**) were characterized by multinuclear NMR and IR spectroscopy and mass spectrometry and the homogeneity of the new compounds was where possible confirmed by microanalysis. Solid-state and solution ^{77}Se and ^{125}Te NMR spectroscopic data can be found in Table 1.

The respective acenaphthene NMR signals for compounds **9**, **10** and **13** display an upfield shift, lying at lower chemical shifts, indicating the nuclei are more shielded than in equivalent naphthalene salts **3**, **1** and **4**, respectively. The ^{125}Te NMR spectrum of **10** is comparable with the data reported for the naphthalene telluronium salt **1** by Furukawa *et al.*;[30] two peaks at δ = 641.1 ppm (Te^+) and δ = 521.6 ppm (Te), each peak exhibiting satellites due to ^{125}Te-^{125}Te coupling. Indication of a strong through-space *peri*-interaction is observed between the telluronio and tellurenyl groups, with large coupling constants (J_{TeTe} = 945.8 Hz) of a similar magnitude to the reported naphthalene derivative (**1** J_{TeTe} = 1093 Hz[30]).

In contrast, the significantly smaller *J* values observed for ^{77}Se-^{77}Se coupling [**3** (166.9 Hz); **9** (140.7 Hz)] in the ^{77}Se NMR spectra for analogous selenonium salts **3** [δ = 435.9 ppm (Se^+), δ = 391.8 ppm (Se)] and **9** [δ = 422.3 ppm (Se^+), δ = 365.7 ppm (Se)] implies a weaker through-space interaction is occurring in each case. A more direct comparison is possible through the corresponding reduced coupling constants K, which decrease by *ca.* 60% on going from **1** (K = 9.0.1021 $kgm^{-2}s^{-2}A^{-2}$) to **3** (K = 3.8.1021 $kgm^{-2}s^{-2}A^{-2}$). As might be expected, the mixed telluronio-selanyl compounds **4** and **13** display properties in between those of the bis-tellurium and bis-selenium analogues. The reciprocal ^{125}Te NMR and ^{77}Se NMR spectra for both compounds exhibit single peaks [**4** δ_{Te} = 705.7 ppm, δ_{Se} = 346.9 ppm; **13** δ_{Te} = 679.2 ppm, δ_{Se} = 322.6 ppm] with satellites attributed to ^{125}Te-^{77}Se coupling. The relatively large *J* values [**4** (428.9 Hz); **13** (381.5 Hz)], lying between those of the telluronium salts (**1**, **10**) and selenonium salts (**3**, **9**), indicate a potential weakly-attractive through-space interaction.

Solid-state NMR spectra were recorded for compounds **A9**-**A13** and **9**-**13**, and chemical shifts are found to be close to the solution state values. It was not possible to determine *J* values owing to the larger line widths obtained in the solid-state NMR spectra. The deviations of up to 17.8 ppm for ^{77}Se and 62.8 ppm for ^{125}Te between the solution-state and solid-state chemical shifts result from the changes in geometry imposed by the crystal structure in the solid state. DFT calculations of ^{77}Se and ^{125}Te NMR parameters were performed on fully geometry-optimized structures (full details are given in the ESI). These enabled assignment of solid-state NMR spectra which contain more than one resonance. For compounds **A9** and **A10**, the two chemically-equivalent selenium and tellurium atoms in each of the molecules are crystallographically-inequivalent in the solid state owing to the conformation of the molecule. This results in the observation of two ^{77}Se and ^{125}Te distinct resonances in the solid-state NMR spectra for each compound. For the crystallographically-inequivalent sites in these compounds, the experimental chemical shift differences of 51.6 ppm (^{77}Se) and 114.3 ppm (^{125}Te) for **A9** and **A10** show reasonable agreement with differences 35.5 ppm and 135.6 ppm predicted

Table 2. Torsion angles [°] categorizing the aryl moiety conformations in 2-13 [values in parentheses are for independent molecules]

Compound	*Methyl group conformations*	*Naphthalene ring conformations*		*Phenyl ring conformations*	
Torsion angle	C(10)-C(1)-E(1)-C(17)	C(10)-C(1)-E(1)-C(11)	C(10)-C(9)-E(2)-C(18)	C(1)-E(1)-C(11)-C(12)	C(9)-E(2)-C(18)-C(19)
2	θ_1 107.45(1)	θ_2 -143.70(1)	θ_3 83.14(1)	γ_1 -85.88(1)	γ_2 -168.50(1)
	Me_1: axial	$Acenap_1$: twist	$Acenap_2$: axial	Ph_1: axial	Ph_2: equatorial
3	θ_1 172.45(1)	θ_2 -86.98(1)	θ_3 123.55(1)	γ_1 -27.60(1)	γ_2 -73.43(1)
	Me_1: equatorial	$Acenap_1$: axial	$Acenap_2$: twist	Ph_1: equatorial	Ph_2: axial
4	θ_1 -166.17(1)	θ_2 101.53(1)	θ_3 -95.24(1)	γ_1 -162.60(1)	γ_2 139.24(1)
	Me_1: equatorial	$Acenap_1$: axial	$Acenap_2$: axial	Ph_1: equatorial	Ph_2: twist
Compound	*Methyl group conformations*	*Acenaphthene ring conformations*		*Phenyl ring conformations*	
Torsion angle	C(10)-C(1)-E(1)-C(19)	C(10)-C(1)-E(1)-C(13)	C(10)-C(9)-E(2)-C(20)	C(1)-E(1)-C(13)-C(14)	C(9)-E(2)-C(20)-C(21)
5	θ_1 -161.22(1) [174.72(1)]	θ_2 -93.08(1) [-79.48(1)]	n/a	γ_1 146.13(1)	n/a
	Me_1: equatorial	$Acenap_1$: axial		Ph_1: twist	
6	θ_1 -175.11(1)	θ_2 -75.87(1)	n/a	γ_1 160.24(1) [142.73(1)]	n/a
	Me_1: equatorial	$Acenap_1$: axial		Ph_1: axial	
7	θ_1 158.97(1)	θ_2 -63.80(1)	n/a	γ_1 42.76(1)	n/a
	Me_1: equatorial	$Acenap_1$: axial		Ph_1: twist	
8	θ_1 174.52(1) [-176.50(1)]	θ_2 70.14(1) [-71.43(1)]	θ_3 84.25(1) [-77.17(1)]	γ_1 36.73(1) [152.63(1)]	γ_2 17.74(1) [152.74(1)]
	Me_1: equatorial	$Acenap_1$: axial	$Acenap_2$: axial	Ph_1: twist	Ph_2: equatorial
9	θ_1 168.18(1)	θ_2 -92.93(1)	θ_3 86.79(1)	γ_1 152.07(1)	γ_2 179.14(1)
	Me_1: equatorial	$Acenap_1$: axial	$Acenap_2$: axial	Ph_1: equatorial	Ph_2: equatorial
10	θ_1 -171.91(1)	θ_2 94.31(1)	θ_3 85.65(1)	γ_1 151.07(1)	γ_2 176.55(1)
	Me_1: equatorial	$Acenap_1$: axial	$Acenap_2$: axial	Ph_1: equatorial	Ph_2: equatorial
11	θ_1 -172.30(1) [172.31(1)]	θ_2 -72.85(1) [71.84(1)]	θ_3 -82.27(1) [70.36(1)]	γ_1 139.82(1) [27.27(1)]	γ_2 164.89(1) [-155.58(1)]
	Me_1: equatorial	$Acenap_1$: axial	$Acenap_2$: twist	Ph_1: equatorial	Ph_2: equatorial
12	θ_1 166.49(1)	θ_2 70.56(1)	θ_3 76.93(1)	γ_1 -130.73(1)	γ_2 -160.11(1)
	Me_1: equatorial	$Acenap_1$: axial	$Acenap_2$: axial	Ph_1: twist	Ph_2: equatorial
13	θ_1 -169.37(1) [169.90(1)]	θ_2 -72.56(1) [74.63(1)]	θ_3 -80.86(1) [71.69(1)]	γ_1 139.89(1) [23.03(1)]	γ_2 -15.29(1) [25.75(1)]
	Me_1: equatorial	$Acenap_1$: axial	$Acenap_2$: axial	Ph_1: equatorial	Ph_2: equatorial

[a] Nap1/Acenap1: naphthalene/acenaphthene ring E(1); [b] Nap2/Acenap2: naphthalene/acenaphthene ring E(2); [c] Ph1: E(1) phenyl ring; [d] Ph2: E(2) phenyl ring; [e] axial: perpendicular to C(ar)-E-C(ar) plane; [f] equatorial: coplanar with C(ar)-E-C(ar) plane; [g] twist: intermediate between axial and equatorial.[6,2]

by the calculations. The crystal structures of compounds **11** and **13** contain two crystallographically-distinct molecules per asymmetric unit. For compound **11**, only one isotropic resonance was observed in the ^{77}Se solid-state NMR spectrum. We note that the two distinct selenium species in the structure have very similar local bonding geometries, and the DFT calculations predict only a 7.5 ppm difference in chemical shift between the two sites.

Furthermore, DFT calculations performed on a structure for which only hydrogen positions were optimized predict a smaller chemical shift difference of 3.8 ppm. Therefore it is likely that the two distinct selenium sites are unresolved in the experimental solid-state ^{77}Se NMR spectrum, where a line width of 5 ppm was obtained. For compound **13**, two ^{77}Se and two ^{125}Te resonances are observed in the experimental solid-state ^{77}Se and ^{125}Te NMR spectrum, indicating larger structural differences between the two molecules in the asymmetric unit.

This could be related to the larger difference in phenyl ring conformation between the two molecules in the crystal structure for **13** (Table 2), which is known to be an important factor in determining ^{77}Se chemical shifts.[31,32] Indeed, the structural differences between the two crystallographically-distinct molecules are reflected in the DFT calculations which predict chemical differences of 19.0 ppm (^{77}Se) and 10.7 ppm (^{125}Te).

X-ray investigations: Suitable single crystals were obtained for **2-14** by diffusion of hexane into saturated solutions of the individual compound in dichloromethane. Compounds **2-4**, **6**, **7**, **9**, **10**, **12**, and **14** crystallise with one molecule in the asymmetric unit, compounds **5**, **8**, **11** and **13** contain two nearly identical molecules in the asymmetric unit. Selected interatomic torsion angles are listed in Tables 2 and 3. Further crystallographic information including bond lengths and angles, Hydrogen-bond and non-conventional weak inter- and intra-molecular interaction data can be found in Tables S2-S6 in the Electronic Supporting Information (ESI).

The molecular structures of chalconium monocation salts **2-13** exhibit a range of structurally diverse configurations which are notably different to those of the respective parent derivatives **N2-N4**,[23] **A5-A13**.[27] A general increase in the *peri*-separation is observed for molecules accommodating heavier heteroatoms in the proximal *peri*-positions, but naphthalene salts **2-4** naturally display less molecular distortion and shorter *peri*-distances com-

pared with analogous acenaphthene derivatives **8**, **9** and **13** respectively. Whilst methylation alters the structural architecture of the chalconium salts, the degree of molecular distortion occurring in the organic backbone is comparable to the parent compounds, with no significant change in steric strain upon the introduction of the methyl functional group.

The final solid state structure is governed by weak non-covalent interactions which have an influence on crystal packing and molecular geometry, but the conformation of the aromatic ring systems and subsequent location of p-type lone-pairs dominates the geometry of the *peri*-region. The absolute configuration of the aromatic ring systems and methyl functionality in **2-13** can be classified by the relative alignment of the naphthalene and acenaphthene backbones and the aryl moieties with respect to the C(ar)-E-C(ar) planes.[6,23,25,27,29] This is calculated from torsion angles θ and γ [Table 2; Figure 2] which define the rotation of the aryl groups around the E-$C_{Nap/Acenap}$ bonds and E-C_{Ph} bonds, respectively. When θ approaches 90°, the orientation is denoted axial; the respective E-C_{Ar} bond aligns perpendicular to the mean least-squares plane and corresponds to a type A structure.[6,27,29] Correspondingly, the type B conformation aligns the E-C_{Ar} bond in an equatorial position, *quasi*-planar and with angle θ approaching 180°. For values of θ which lie out with those of an axial or equatorial structure (~135°), the classification is denoted twist and corresponds to type C.[6,27,29]

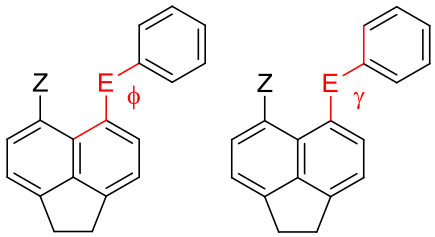

Figure 2. The absolute conformation of aromatic rings and methyl functionalities is calculated from torsion angles θ (defining rotation around the E-C_{Acenap} bond) and γ (defining rotation around the E-C_{Ph} bond).[6,27,29]

The conformation of monocation **2** can accordingly be classified as type A-CAc; a perpendicular alignment of the methyl group with respect to the mean naphthalene plane [θ1 = 107.45(1)°] corresponds to type A,[6,29] whilst twist [S(1)] and axial [S(2)] arrangements of the phenyl rings, displaced to the same side of the naphthalene plane, correspond to CAc (c denotes a cis orientation of phenyl rings with respect to the mean naphthalene plane; Figures 3 and 4).

The substitution of the heavier chalcogens imposes a contrasting geometry on **3** and **4**, aligning the E-C_{Me} bond in an equatorial position along the naphthyl plane (type B)[6,29] and promoting a *cis* orientation of phenyl moieties to afford B-ACc and BAAc type conformations, respectively (Table 2, Figures 3 and 4). The geometrical constraints associated with the equatorial positioning of the methyl group generates a *quasi*-linear three-body fragment of the type E···E`-C_{Me}, which may promote the delocalization of a chalcogen lone-pair (G) to the antibonding σ* (E-C) orbital, thus forming an attractive three-center four-electron (3c-4e) type interaction.[6,27] Evidence for this is supported by short non-bonded *peri*-distances, ~20% shorter than the respective sum of van der Waals radii (Σr_{vdW}) [**3** 3.077(3) Å; **4** 3.177(1) Å] and E···E`-C_{Me} angles which approach 180° [**3** ψ = 177.1°; **4** ψ = 171.2°]. No similar alignment is found in **2**, with the A-CAc conformation accounting for a more acute S(2)···S(1)-C(17) angle of ψ = 100.7° and a larger relative *peri*-separation than might be expected from interactions between lighter Group 16 congeners [3.006(2) Å: 84%].

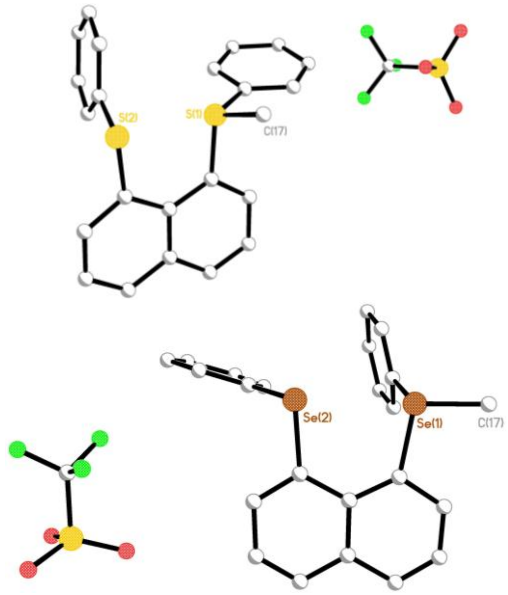

Figure 3. The molecular structures of naphthalene chalconium salts 2 (top) and 3 (bottom; H atoms omitted for clarity). The structure of 4 (adopting a similar conformation to 3) is omitted here but can be found in the ESI (Figure S3).

In all three derivatives the chalcogen moieties are accommodated by the elongation of C-C bonds around C10 (mean 1.43 Å; *cf.* C5 bonds: 1.42 Å) and supplemented by an increase in the C1-C10-C9 angular splay (mean 127°; *cf.* C4-C5-C6: 120°). Additional relaxation is afforded by the displacement of the *peri*-atoms to opposite sides of the naphthyl plane (0.2-0.5 Å) and the divergence of the exocyclic bonds (splay angles 13.1-14.2°). Considerable buckling of the usually rigid naphthalene unit is also observed with central C-C-C-C torsion angles deviating from planarity by 2-6°.

The *cis* orientation exhibited by each compound encourages the association of neighboring phenyl ring systems through intramolecular non-bonded π-π stacking (Figure 5). The mutual equatorial (γ ~180°)-axial (γ ~90°) conformation (with respect to the C_{Nap}-E-C_{Ph} planes) in **2** and **3** and the equatorial-twist (γ ~135°) configuration in **4** arranges the aromatic rings in an edge- (point-) to-face motif (T-shaped) as a result of weak CH···π type interactions[33] [CH···Cg **2** 2.919(1) Å; **3** 2.613(1) Å; **4** 2.650(1) Å; within the range for typical CH···π edge-to-face π-stacking ~3.0 Å; Figure 5].[34]

Additional weak intermolecular CH···π interactions are present in **2** and **3** connecting naphthalene and phenyl rings of neighboring molecules [CH···cg 2.80-2.92 Å; Figure S1, ESI], whilst weak CF···π interactions in **2** and **4** connect adjacent aromatic and triflate moieties [CF···cg 3.45-3.83 Å; Figure S1, ESI]. The triflate anions also interact with the naphthalene molecule via a number of non-conventional CH···O and CH···F type hydrogen-bonds [CH···O 2.31–2.58 Å; CH···F 2.48-2.54 Å; Figure S1, ESI].

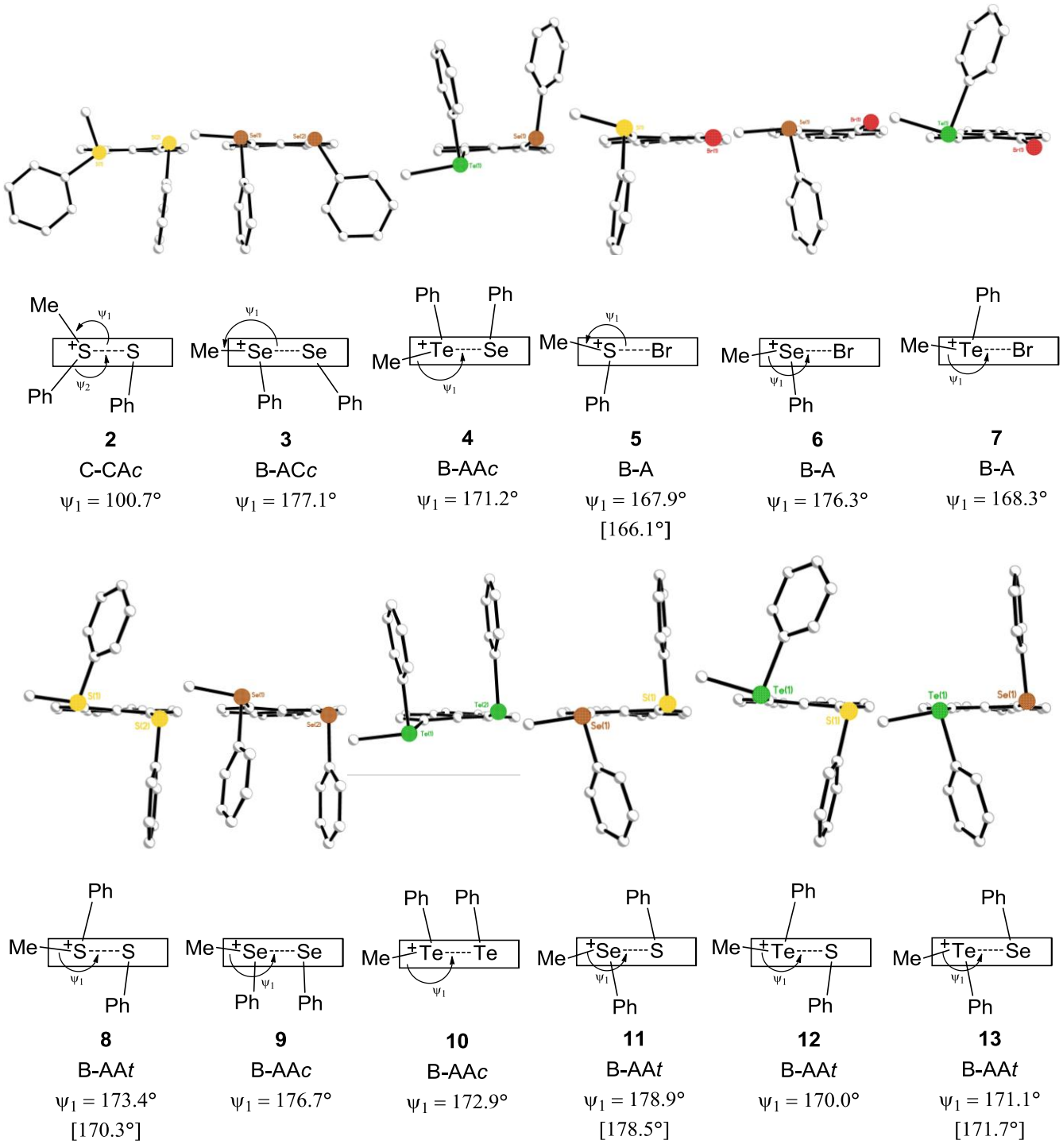

Figure 4. The relative configuration of methyl and E(phenyl) groups, the *quasi*-linear arrangements and structural classification of 2-13.

The introduction of the ethane linker on the acenaphthene organic framework naturally increases the splay of the exocyclic bonds resulting in larger *peri*-separations compared to equivalent naphthalene compounds.[27] In the acenaphthene systems **5-13** partial relief of *peri*-space crowding is also achieved by an increase in the C1-C10-C9 bay-angles, which splay to a mean 131° compared with the ideal 127°. Further deformation of the acenaphthene geometry is achieved by the elongation of bonds around C5 (average lengths 1.47 Å *cf*. 1.42 Å) and C10 (average lengths 1.44 Å *cf*. 1.42 Å), with the central C5-C10 bond stretching from 1.39 Å to an average of 1.42 Å. Nevertheless, the presence of the ethane bridge ensures the C4-C5-C6 bond angle remains close to ideal (average 111.4° compared with the ideal 111.3°).

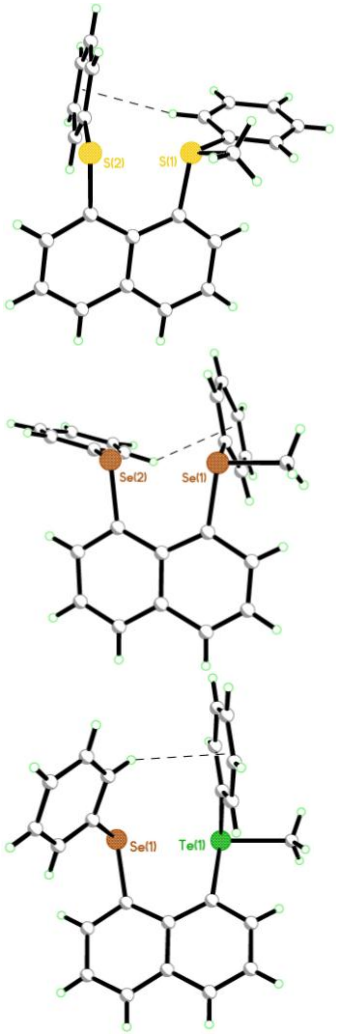

Figure 5. Intramolecular edge-to-face π-π stacking in 2-4 as a result of weak hydrogen bond type CH···π interactions.

The series of 5-bromo-6-(methyl)(phenyl)chalconium acenaphthenes **5-7** adopt a similar equatorial-axial arrangement (Figure 6), positioning the E-C_{Me} bond close to the acenaphthene plane and subsequently forcing the E-C_{Ph} bond to lie with a perpendicular configuration (type B-A; Figure 4). The location of the methyl functionality provides the correct geometry for the existence of a *quasi*-linear three-body Br···E-C_{Me} fragment with potential 3c-4e character [Br···E-C angles (ψ) in the range 166-176°; Figure 4]. Naturally, the non-bonded Br···E *peri*-distances display a general increase with increasing chalcogen size, with separations lengthening from 3.181(3) Å [3.182(3) Å] in **5** to 3.2848(14) Å in **7**, but still 13-16 % shorter than the sum of van der Waals radii in each case.

The natural bond stretching and angle widening distortions of the acenaphthene framework are insufficient to completely alleviate the steric strain imposed by the substitution of bulky chalcogen and halogen substituents in **5-7**. Supplementary displacement of the *peri*-atoms away from the acenaphthene mean plane and a greater divergence of the exocyclic bonds transpire to help alleviate *peri*-space crowding. Considerable distortion is observed within the bay-region, with large, but comparable angular splays observed for the E-C_{Acenap} and X-C_{Acenap} bonds [**5** 17.2° [16.3°]; **6** 17.8°; **7** 17.2°]. The disposition of the *peri*-atoms to opposite sides of the acenaphthene ring ranges from 0.1-0.9 Å and further deformation is achieved by a minor buckling of the acenaphthene framework (central torsion angles 1-4°). In all three compounds, adjacent acenaphthene molecules are connected via intermolecular CH···π interactions [2.79-2.88 Å], with sulfur derivative **5** exhibiting two additional short C-Br···π type contacts [3.62-3.95 Å; Table S1]. Further intermolecular interactions link neighboring acenaphthene and triflate moieties in each structure, with non-conventional hydrogen-bonding dominating the short contacts [CH···O 2.20-2.60 Å; CH···F 2.45-2.51 Å].

The structures of chalconium salts **9** and **10**, prepared from 5,6-bis(phenylselanyl)acenaphthene **A9** and 5,6-bis(phenyltelluro)acenaphthene **A10**, adopt a similar configuration of aromatic rings and methyl functionalities to the TeSe naphthalene derivative **4** (B-AAc; Figures 4 and 7). In contrast, the acenaphthene bis-sulfur compound **8** and the group of mixed chalcogen derivatives **11-13**, assume a B-AAt type configuration (Figures 4 and 7), again positioning both S-C_{Ph} bonds perpendicular to the mean acenaphthene plane, but displacing the phenyl rings to opposite sides of the molecule (*t* corresponding to a trans orientation of phenyl groups with respect to the acenaphthene plane). The geometrical constraints of the two B-AA type conformations adopted by **8-13**, affords a *quasi*-linear three-body fragment of the type E···E`-$C_{Me}$ which provides a potentially attractive 3c-4e component for the E···E` interaction. In all cases ψ approaches 180° [170-177°], and non-bonded *peri*-distances are 16-19% within the sum of van der Waals radii for the two interacting chalcogen atoms [**8** 3.093(3) Å (3.034(3) Å); **9** 3.2469(19) Å; **10** 3.445(3) Å; **11** 3.114(3) Å (3.073(4) Å); **12** 3.117(3) Å; **13** 3.2089(14) Å (3.1718(14) Å)].

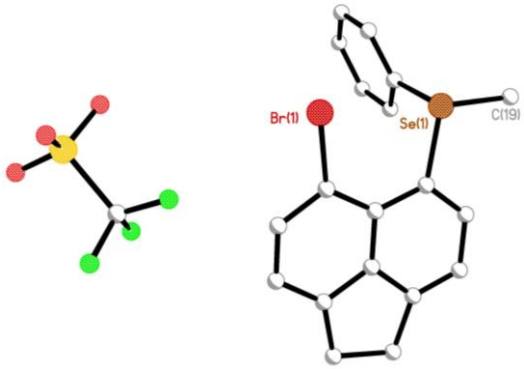

Figure 6. The molecular structure of chalconium salt 6 (H atoms omitted for clarity). The structures of 5 and 7 (adopting conformations similar to 5) are omitted here but can be found in the ESI (Figure S4).

In line with parent compounds **A8-A13**,[27] deformation of the natural acenaphthene geometry in **8-13** through in-plane and out-of-plane distortions and buckling of the carbon skeleton generally increases as larger atoms occupy the proximal 5,6-positions. A notable increase in the *peri*-separation is observed as the heavier congeners are substituted, with a marked lengthening from 3.093(3) Å (3.034(3) Å) in **8** to 3.445(3) Å in **10**. The increased congestion of the *peri*-space causes a greater divergence of the E-C_{Acenap} bonds within the acenaphthene plane with large positive splay angles in the range 13.2°-19.9°. Out-of-plane distortion is comparable in all five compounds, with the

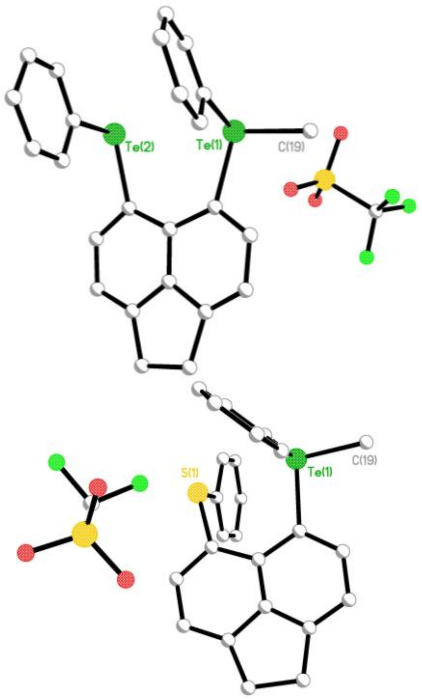

Figure 7. The molecular structures of chalconium salts 10 and 12 (H atoms omitted for clarity). The structures of 8, 9, 11 and 13 (adopting conformations similar to 10 and 12) are omitted here but can be found in the ESI (Figure S5).

peri-atoms displaced to opposite sides of the mean acenaphthene plane by 0.1-0.4 Å. The deviation of the acenaphthene framework away from planarity is also consistent throughout the series with central C-C-C-C torsion angles within 1-6°. All members of the group exhibit short intermolecular forces; in each case CH···π [2.41-2.99 Å] interactions connect adjoining aromatic rings and CH···O [2.36-2.58 Å] and CH···F [2.37-2.55 Å] hydrogen-bonding associate triflate counter-anions with the organic framework.

Treatment of 5,6-bis(phenyltelluro)acenaphthene **A13** with two molar equivalents of MeOTf resulted in the methylation of both tellurium centers, affording the dication salt [{Acenap(TePh)$_2$(Me)$_2$}$^{2+}$(OTf)$_2$] **14** (Figure 8). The substitution of large tellurium moieties constrained at the close sub-van der Waals *peri*-positions cramps the bay-region leading to an increase in steric pressure arising from non-bonded interactions due to a direct overlap of the Te orbitals. The additional electrostatic repulsion acting between the positively charged cationic tellurium centers enhances the steric strain within the *peri*-region and leads to a greater deformation of the acenaphthene carbon framework. The repulsive Te$^+$···Te$^+$ Coulombic interaction is predominantly accommodated by a greater in-plane divergence of the exocyclic Te-C$_{Acenap}$ bonds [splay angle: 14 23.4°; 10 19.9°], which leads to an increase in the non-bonding Te$^+$···Te$^+$ separation [3.5074(16) Å] compared with the telluronio-tellurenyl Te$^+$···Te separation in monocation **10** [3.445(3) Å]. Nevertheless, the Te$^+$···Te$^+$ separation in **14** [3.5074(16) Å] is still 15% shorter than twice the van der Waals radii for Te [4.12 Å].[35]

The conformation of dication **14** can be classified as type C-CC*c*-C (Figure 9, Table 3). The two Te-C$_{Me}$ bonds are displaced 151.14(1)° and 136.01(1)° from the respective C(10)-C(1)-Te-C$_{Me}$ planes, locating the methyl groups at positions in between an equatorial and axial configuration, corresponding to a twist conformation. The two methyl groups subsequently point away from the center of the molecule and are located on opposite sides of the acenaphthene ring. The CC-*cis* orientation of the two Te-C$_{Ph}$ bonds aligns the two phenyl rings on the same side of the acenaphthene ring and encourages the association of neighboring phenyl ring systems. Nevertheless the cg···cg distance [3.92 Å] is out-with the range for typical π···π stacking [3.3-3.8 Å].[36]

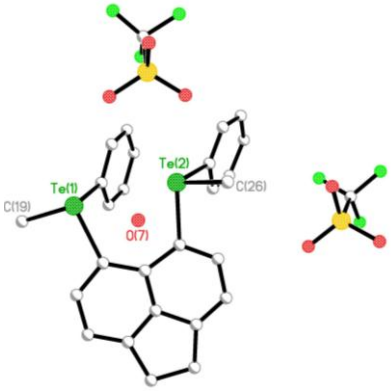

Figure 8. The molecular structure of dication chalconium salt 14 (H atoms omitted for clarity).

Amassing the bulk of the substituents on one side of the molecule ("top half" in Figure 9) leaves much open space on the other. In the solid, this space is actually occupied by a water molecule (see Figure 8), presumably introduced during the workup in air. Crystallization under anhydrous conditions affords the same structure of the dication of **14**, now with an O atom from one of the triflate counter ions at the position of this water (the "anhydrous" structure still contains one water molecule per two structural units, but this is more remote from the Te atoms).

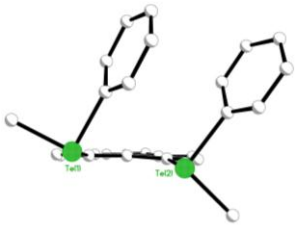

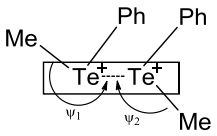

14
C-CC*c*-C
ψ_1 = 160.5°
ψ_2 = 143.8°

Figure 9. The relative configuration of methyl and Te(phenyl) groups and structural classification of 14.

To assess the role of this water molecule, density functional theory (DFT) calculations were performed. When an optimization is started for the pristine dication from the crystal structure, a B-AB-A-type minimum is obtained (top of Figure 10), reminiscent of related neutral bis(phosphines).[37] When the water molecule is retained, a noticeably different conformation is obtained (bottom of Figure 10), about halfway between the pristine minimum and the structure observed in the solid (note that dispersion forces favoring π-stacking are not accounted for at the level used).

Table 3. Torsion angles [°] categorizing the aryl moiety conformations in 14.

Methyl group conformations	
C(10)-C(1)-Te(1)-C(19)	C(10)-C(1)-Te(2)-C(26)
151.14(1): Me1: equatorial	136.01(1): Me2: twist
Acenaphthene ring conformations	
C(10)-C(1)-Te(1)-C(13)	C(10)-C(9)-Te(2)-C(18)
57.05(1): Acenap1: twist	-125.83(1): Acenap2: twist
Phenyl ring conformations	
C(1)-Te(1)-C(13)-C(14)	C(9)-Te(2)-C(18)-C(19)
37.22(1): Ph1: twist	17.79(1): Ph2: twist

The water is held in a position not too far from where it is found in the solid, though not approaching the Te atoms quite as closely (see the distances on the bottom of Figure 10). In the starting structure, one of the H atoms of the water (which were not refined in the X-ray analysis) was placed pointing toward the lone pair of the more distant Te atom, but rotated away during optimization. In the gas phase, this water molecule is bound rather strongly (with a raw binding energy exceeding 40 kcal/mol at the B3LYP level), and mostly through electrostatic interactions between the positively charged Te atoms (+1.4e according to natural population analysis) and the negatively charged O atom.

Figure 11 displays the relationship between *peri*-distance versus collective *peri*-atom size (sum of van der Waals radii of the two *peri*-atoms) for acenaphthene chalconium salts **5-13**. Geometric constraints imposed by the rigidity of the acenaphthene backbone places greater steric pressure on systems incorporating larger heteroatoms within sub-van der Waals radii at the proximal *peri*-positions. Naturally, when larger halogen or chalcogen congeners occupy the close 5,6-positions, increasing non-bonding interactions result as a direct consequence of the overlap of orbitals. The acenaphthene framework subsequently distorts to alleviate the steric strain leading to a general increase in the *peri*-separation (Figure 11).

Nevertheless, the relative conformation of the aromatic moieties dictates the location of the chalcogen and halogen p-type lone-pairs, influencing the degree of orbital overlap and governing the geometry of the *peri*-region. The molecular configuration can therefore influence the degree to which halogen or chalcogen frontier orbitals take part in attractive or repulsive interactions, resulting in irregular non-bonded *peri*-separations with respect to the size of the interacting atoms.

Counterintuitively, the Se···Se *peri*-distance in **9** [3.2469(19) Å; Σr_{vdW} 3.80 Å[35]], is longer than the Te···E distances found in **12** [3.117(3) Å; Σr_{vdW} 3.86 Å[35]] and **13** [3.2089(14) Å (3.1718(14) Å); Σr_{vdW} 3.96 Å[35]], accommodating heavier chalcogen congeners. Similarly, the S···Br distance in **5** [3.182(3) Å (3.181(3) Å); Σr_{vdW} 3.65 Å[35]] is longer than the Se···S distance in **11** [3.114(3) Å (3.073(4) Å); Σr_{vdW} 3.70 Å[35]] and the Te···Br distance in **7** [3.2848(14) Å; Σr_{vdW} 3.91 Å[35]] is longer than the Te···Se distance in **13** [3.2089(14) Å (3.1718(14) Å); Σr_{vdW} 3.96 Å[35]]. This appears to be correlated to the contrasting conformation of the *cis* and *trans* B-AA type systems in **8-13** and the B-A configuration prevalent for compounds **5-7**. Greater lone pair-lone pair repulsion is observed in compounds adopting type B-AAc and B-A configurations, with larger than expected *peri*-distances relative to the size of the interacting atoms (Figure 11). Lone-pair interactions are less effective when the *peri*-moieties adopt a B-AAt conformation. For both the type B-AAc/B-A and type B-AAt groups, *quasi*-linear relationships may be observed between *peri*-distance and *peri*-atom size (Figure 11).

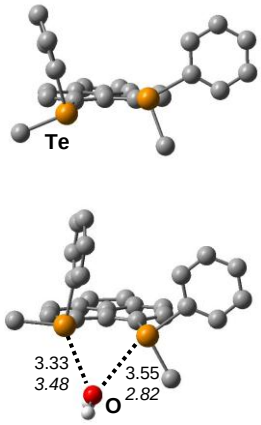

Figure 10: B3LYP optimized bare dication from 14 (top) and with one water molecule added (bottom), including selected bond distances in Å (in italics: from X-ray crystallography, *cf.* Figure 9); organic H-atoms omitted for clarity.

To complement these findings, additional DFT calculations were performed for acenaphthene derivatives **8-13**, comparing the *cis* and *trans* B-AA type conformations and determining the extent of three-center, four-electron type interactions occurring in the series. Table 4 summarizes selected geometrical parameters for **8-13**, together with the chalcogen-chalcogen Wiberg bond indices (WBIs).[38] The latter are a probe for the extent of covalent bonding, approaching a value close to one for true single bonds.

The atomic coordinates obtained from X-ray crystallography were reoptimised at the B3LYP level to ensure that the chosen basis sets and effective core potentials (ECPs) are adequate for the problem at hand. Interestingly, the optimized *peri*-distances between the chalcogens are noticeably shorter than those observed in the solid, by up to 0.08 Å (overestimation is usually a common DFT problem). Nevertheless, this appears systematic as an excellent linear correlation is found between DFT and X-ray distances, with a slope of 0.88 and a correlation coefficient of 0.96.

In order to assess the difference between the *cis* and *trans* structural motifs, a conformational search was undertaken where all molecules **8-13** were optimized in the respective other conformation. In each case the two possible B-AA conformations were considered, with the phenyl groups adopting either the *cis* (B-AA*c*) or the *trans* (B-AA*t*) orientation. It is interesting to note that AA*c* conformations could be optimized for all members of the group, contrasting with a similar study of the parent compounds **A8-A13** which invariably optimized to AB forms (or intermediate structures denoted AC or CC, where one or both of the dihedral angles θ are close to 140°; Figure 2).

In all cases the most stable conformer corresponded to the B-AA*t* configuration, but the energy span between the two conformations is remarkably small, ranging from 3.7 kJ/mol for **8** to 7.1 kJ/mol for **10** (Table 4). The formation of the B-AA*c* conformer for **9** and **10** in the solid is likely to be due to intermolecular interactions or packing forces. When the phenyl

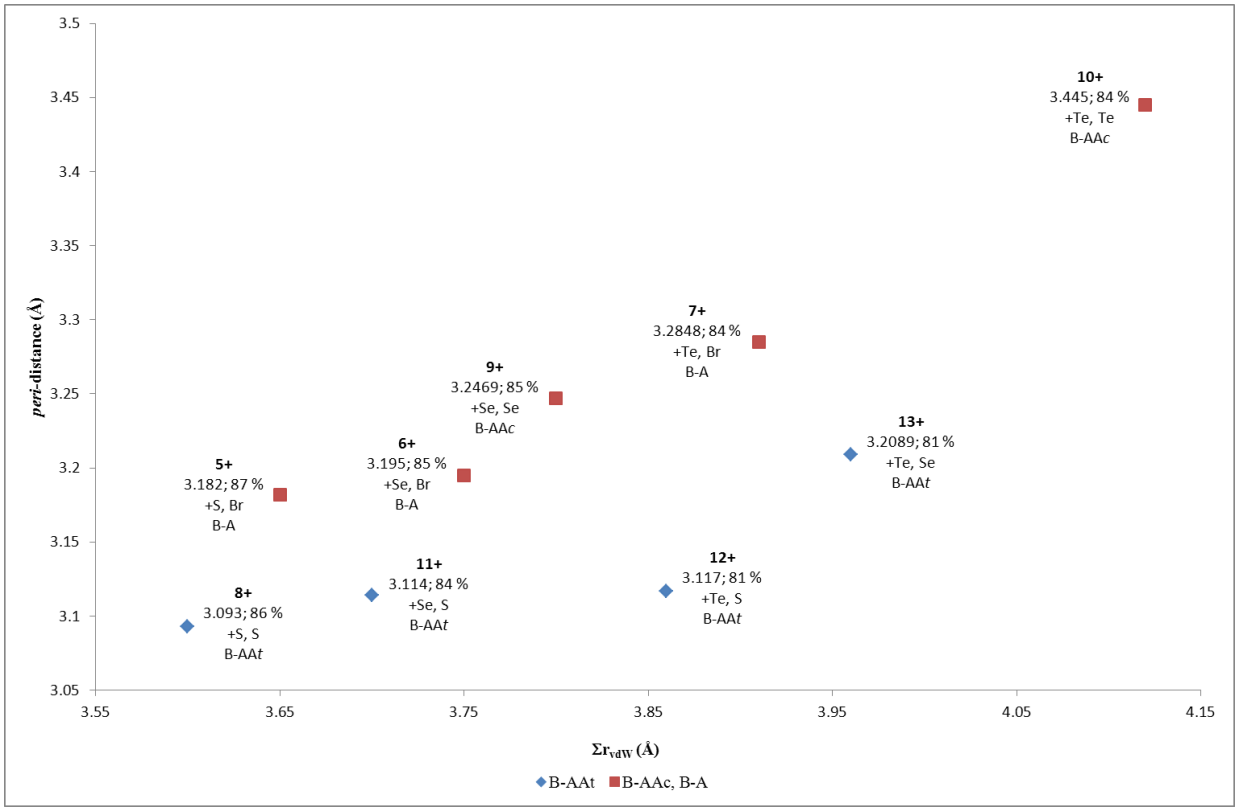

Figure 11. The relationship between the size of the heteroatoms positioned at the 5,6-positions in acenaphthene (sum of van der Waals radii) versus the *peri*-distance in 5-13

substituents are moved from a *cis* orientation to a *trans* orientation, a small decrease in the *peri*-distance is observed. The extent of this decrease ranges from 0.002 Å for **8** to 0.031 Å for **10** (Table 4) and is more pronounced as the size of the interacting *peri*-atoms increases. The extent of covalent bonding in **8-13** was investigated to assess whether the change in *peri*-distance with conformation is a result of specific bonding interactions. The Wiberg bond index (WBI), which usually approaches a value of one for a true single bond, was investigated for each conformer in the series (**8-13**).

In general, there is a trend to higher WBIs as large atoms occupy the proximal *peri*-positions, independent of the conformation of the aromatic rings. In all cases, WBIs for the B-AA*t* conformer are slightly greater than for the equivalent B-AA*c* structure by 0.004-0.011 units. As expected, very small WBIs [0.052/0.041] are computed for the two conformers of **8** with a relatively large *peri*-distance [86% Σr_{vdW}] between the two small sulfur substituents. Significantly higher values are obtained for the heavier members of the series with WBIs in the range 0.102 (**9** SeSe) - 0.184 (**10** TeTe) indicating the onset of weak three-center, four-electron type interactions, which become more prevalent as heavier congeners are introduced along the series. In the second-order perturbation analysis of the natural bond orbitals (NBOs)[39] of **10**, weak donor-acceptor interactions are apparent, involving the p-type lone pair on the TePh group and the σ^*(Te-CH_3) antibonding orbital on the other side. These interactions amount to *ca*. 60 kJ/mol, similar to the findings for the neutral precursor **A10**.[27] Unsurprisingly, significantly lower WBIs are obtained for the dication **14** (0.046) and its water adduct (0.039), *cf*. Figure 10.

These findings correlate with the ^{77}Se and ^{125}Te NMR data and *J* coupling values. Considering the ^{125}Te solid-state chemical shifts for compounds **10**, **12** and **13**, a systematic decrease in chemical shift of the Te^+ species is observed as heavier congeners are introduced on the adjacent *peri* site. This indicates that as the adjacent atom becomes heavier, the Te^+ species becomes more shielded due to increasing through-space lone-pair interactions between the two chalcogen congeners. Similarly, the ^{77}Se chemical shift for the Se^+ species in compound **9** is also lower than that for compound **11**, indicating that through-space interactions are increased for compound **9** which contains the heavier congener on the adjacent *peri* site. These observations are mirrored in the ^{77}Se and ^{125}Te solution-state NMR chemical shifts which follow the same trend, and the evidence for through-space interactions is supported by the *J* coupling values which are substantially larger for compounds containing heavier chalcogen pairs.

CONCLUSION

Naphthalene compounds [Nap(EPh)(E` Ph)] (Nap = naphthalene-1,8-diyl; E/E` = S, Se, Te) **N2-N4** and associated acenaphthene derivatives [Acenap(EPh)(E` Ph)] (Acenap = acenaphthene-5,6-diyl; E/E` = S, Se, Te) **A5-A13** have been independently treated with methyl trifluoromethanesulfonate [MeOTf], affording twelve monocation chalconium salts **2-13**. Reac-

tion of bis-tellurium compound **A10** with two equivalents of MeOTf additionally afforded the doubly methylated dication salt $[\{Acenap(TePhMe)_2\}^{2+}\{(CF_3SO_3)_2\}^{2-}]$ **14**. Where a choice exists between potential methylation sites (mixed-chalcogen derivatives, bromo-chalcogen species) reaction occurs preferentially at the least electronegative chalcogen atom or exclusively at the chalcogen atom in the case of the bromine-chalcogen compounds.

The molecular structures of chalconium monocation salts **2-13** adopt a variety of conformations which are notably different to their parent derivatives **N2-N4**, **A5-A13**, previously reported by us. Naturally, introduction of the ethane linker in acenaphthene compounds causes an increase in the splay of the exocyclic bonds with greater deformation within the bay region compared with equivalent naphthalene derivatives. Whilst a general increase in the *peri*-distance is observed when larger atoms occupy the proximal *peri*-positions, the conformation of the aromatic rings and subsequent location of p-type lone-pairs has a significant impact on the geometry of the *peri*-region, with anomalies in *peri*-separations correlated to the ability of the frontier orbitals to take part in attractive or repulsive interactions. Compounds adopting type B-AAc and B-A configurations experience greater lone pair-lone pair repulsion and consequently exhibit larger than expected *peri*-distances relative to the size of the interacting atoms. Lone-pair interactions are less effective when the *peri*-moieties adopt a B-AA*t* conformation.

In all but one of the monocations (**2**), the methyl group locates close to the mean acenaphthene/naphthalene backbone (type B), affording a *quasi*-linear three-body C_{Me}-E···Z (E = Te, Se, S; Z = Br/E) fragment and providing an attractive component for the E···Z interaction. Density-functional studies have confirmed these interactions and suggested the onset of three-center, four-electron type bonding under appropriate geometric conditions, becoming more prevalent as heavier congeners occupy the proximal *peri*-positions. These findings correlate with the ^{77}Se and ^{125}Te NMR data and *J* coupling values. Firstly, a systematic decrease in chemical shift of the Te^+ species is observed in the ^{125}Te solid-state for compounds **10**, **12** and **13**, as heavier congeners are introduced on the adjacent *peri* site; with increasing size of the adjacent heteroatom, the Te^+ species becomes more shielded due to increasing through-space lone-pair interactions between the two chalcogen congeners. A similar result is observed in the ^{77}Se solid-state NMR for the Se^+ species in compounds **9** and **11**; an increased through-space interaction is indicated in **9** which contains the heavier congener on the adjacent *peri* site by a lower chemical shift. These observations are mirrored in the ^{77}Se and ^{125}Te solution-state NMR chemical shifts which follow the same trend. The increasingly large *J* values for Se-Se, Te-Se and Te-Te coupling observed in the ^{77}Se and ^{125}Te NMR spectra for **1**, **3**, **4**, **9**, **10** and **13** give further evidence for the existence of a weakly-attractive through-space interaction.

ASSOCIATED CONTENT

Supporting Information. Full experimental details, Solid State NMR experimental and interpretation, crystallographic analyses and computational details. This material is available free of charge via the Internet at http://pubs.acs.org.

AUTHOR INFORMATION

Corresponding Author

Dr Fergus R. Knight, School of Chemistry, University of St Andrews, St Andrews, Fife, KY16 9ST, U.K; E-mail: frk@st-andrews.ac.uk; Fax: (+44) 1334 463384; Tel: (+44)1334 463829.

ACKNOWLEDGMENT

Elemental analyses were performed by Stephen Boyer at the London Metropolitan University. Mass Spectrometry was performed by Caroline Horsburgh. Calculations were performed using the EaStCHEM Research Computing Facility maintained by Dr. H. Früchtl. The work in this project was supported by the Engineering and Physical Sciences Research Council (EPSRC). Michael Bühl wishes to thank EaStCHEM and the University of St Andrews for support.

REFERENCES

(1) (a) Lewis, G. N.; *Valence and the Structure of Atoms and Molecules*, The Chemical Catalog Co., New York, 1923, ch. 8. (b) Langmuir, I. *Science* **1921**, *54*, 59.

(2) Moss, G. P. *Pure Appl. Chem.* **1996**, *68*, 2193.

(3) (a) Bleiholder, C.; Werz, D. B.; Köppel, H.; Gleiter, R. *J. Am. Chem. Soc.* **2006**, *128*, 2666. (b) Steed, J. W.; Atwood, J. L. *Supramolecular Chemistry*, John Wiley & Sons, Chichester, 2000. (c) Schneider, H. J.; Yatsimirsky, A. *Principles and Methods in Supramolecular Chemistry*, John Wiley & Sons, Chichester, 2000.

(4) (a) Hatch, J. J.; Rundle, R. E. *J. Am. Chem. Soc.* **1951**, *73*, 4321. (b) Rundle, R. E. *J. Am. Chem. Soc.* **1963**, *85*, 112. (c) Rundle, R. E. *J. Am. Chem. Soc.* **1947**, *69*, 1327. (d) Sugden, S. *The Parachor and Valency,* Knopf, New York, 1930, ch. 6. (e) Pimental, G. C. *J. Chem. Phys.* **1951**, *19*, 446. (f) *The Nature of the Chemical Bond,* 3rd ed.; Pauling, L., Ed.; Cornell University Press, Ithaca, New York, 1960, ch. 7. (g) Pauling, L. *J. Am. Chem. Soc.* **1947**, *69*, 542. (h) Coulson, C. A. *d-Orbitals in Chemical Bonding*, in *Proceedings of the Robert A. Welch Foundation Conferences on Chemical Research. XVI. Theoretical Chemistry,* Mulligen, W. O., Ed.; Houston, Texas, 1972, ch. 3. (i) Brill, T. B. *J. Chem. Educ.* **1973**, *50*, 392. (j) Kutzelnigg, W. *Angew. Chem. Int. Ed.* **1984**, *23*, 272. (k) *Valency and Bonding,* Weinhold, F., Landis, C., Eds.; Cambridge University Press, Cambridge, UK, 2005, ch. 3.

(5) For example: (a) Katz, H. E. *J. Am. Chem. Soc.* **1985**, *107*, 1420. (b) Alder, R. W.; Bowman, P. S.; Steel, W. R. S.; Winterman, D. R. *Chem. Commun.* **1968**, 723. (c) Costa T.; Schimdbaur, H. *Chem. Ber.* **1982**, *115*, 1374. (d) Karacar, A.; Freytag, M.; Thönnessen, H.; Omelanczuk, J.; Jones, P. G.; Bartsch, R.; Schmutzler, R. *Heteroat. Chem.* **2001**, *12*, 102. (e) Glass, R. S.; Andruski, S. W.; Broeker, J. L.; Firouzabadi, H.; Steffen, L. K.; Wilson, G. S. *J. Am. Chem. Soc.* **1989**, *111*, 4036. (f) Fuji, T.; Kimura, T.; Furukawa, N. *Tetrahedron Lett.* **1995**, *36*, 1075. (g) Schiemenz, G. P. *Z. Anorg. All. Chem.* **2002**, *628*, 2597. (h) Corriu, R. J. P.; Young, J. C. *Hypervalent Silicon Compounds*, in *Organic Silicon Compounds*, Patai, S., Rappoport, Z., Eds.; John Wiley & Sons Ltd, Chichester, UK, 1989, vol. 1 and 2.

(6) (a) Nakanishi, W.; Hayashi S.; Toyota, S. *Chem. Commun.* **1996**, 371. (b) Nakanishi, W.; Hayashi, S.; Sakaue, A.; Ono, G.; Kawada, Y. *J. Am. Chem. Soc.* **1998**, *120*, 3635. (c) Nakanishi, W.; Hayashi, S.; Toyota, S. *J. Org. Chem.* **1998**, *63*, 8790. (d) Hayashi S.; Nakanishi, W. *J. Org. Chem.* **1999**, *64*, 6688. (e) Nakanishi, W.; Hayashi S.; Uehara, T. *J. Phys. Chem. A* **1999**, *103*, 9906. (f) Nakanishi, W.; Hayashi, S.; Uehara, T. *Eur. J. Org. Chem.* **2001**, 3933. (g) Nakanishi W.; Hayashi, S. *Phosphorus Sulfur Silicon Relat. Elem.* **2002**, *177*, 1833. (h) Nakanishi, W.; Hayashi, S.; Arai, T. *Chem. Commun.* **2002**, 2416. (i) Hayashi, S.; Nakanishi, W. *J. Org. Chem.* **2002**, *67*, 38. (j) Nakanishi, W.; Hayashi, S.; Itoh, N. *Chem. Commun.* **2003**, 124. (k) Hayashi, S.; Wada, H.; Ueno, T.; Nakanishi, W. *J. Org. Chem.* **2006**, *71*, 5574. (l) Hayashi, S.; Nakanishi, W. *Bull. Chem. Soc. Jpn.* **2008**, *81*, 1605.

(7) Bleiholder, C.; Gleiter, R.; Werz, D. B.; Köppel, H. *Inorg. Chem.* **2007**, *46*, 2249.

(8) Bruno, I. J.; Cole, J. C.; Lommerse, J. P. M.; Rowland, R. S.; Taylor, R.; Verdonk, M. L. *Journal of Computer-Aided Molecular Design*, **1997**, *11*, 525.

(9) *Structure Correlation, Vols. 1 and 2*, Bürgi, H. -B., Dunitz, J. D., Eds.; VCH, Weinheim, Germany, 1994.

(10) (a) Pauling, L.; Corey, R. B.; Branson, H. R. *Proc. Natl. Acad. Sci. U.S.A.* **1951**, *37*, 205. (b) Pauling, L.; Corey, R. B. *Proc. Natl. Acad. Sci. U.S.A.* **1951**, *37*, 251. (c) Pauling L.; Corey, R. B. *Proc. Natl. Acad. Sci. U.S.A.* **1951**, *37*, 729.

(11) (a) Desiraju G. R.; Steiner, T. *The Weak Hydrogen Bond*, Oxford University Press, New York, 1999; (b) Steiner, T. *Angew. Chem., Int. Ed.* **2002**, *41*, 48. (c) Steiner, T. *Angew. Chem.* **2002**, *114*, 51.

(12) Nishio, M.; Hirota, M.; Umezawa, Y. *The CH/π-Interaction*, Wiley-VCH, New York, 1998.

(13) (a) Pedireddi, V. R.; Reddy, D. S.; Goud, B. S.; Craig, D. C.; Rae, A. D.; Desiraju, G. R. *J. Chem. Soc., Perkin Trans. 2* **1994**, 2353. (b) Rosenfield, R. E.; Parthasarathy, R.; Dunitz, J. D. *J. Am. Chem. Soc.* **1977**, *99*, 4860. (c) Guru Row, T. N.; Parthasarathy, R. *J. Am. Chem. Soc.* **1981**, *103*, 477. (d) Ramasubbu, N.; Parthasarathy, R. *Phosphorus Sulfur Silicon Relat. Elem.* **1987**, *31*, 221. (e) Glusker, J. P. *Top. Curr. Chem.* **1998**, *198*, 1. (f) Iwaoka, M.; Takemoto, S.; Okada M.; Tomoda, S. *Bull. Chem. Soc. Jpn.* **2002**, *75*, 1611. (g) Corradi, E.; Meille, S. V.; Messina, M. T.; Metrangolo P.; Resnati, G. *Angew. Chem. Int. Ed.* **2000**, *39*, 1782.

(14) (a) Coulson, C. A.; Daudel, R.; Robertson, J. M. *Proc. R. Soc. London Ser. A.* **1951**, *207*, 306. (b) Cruickshank, D. W. *Acta Crystallogr.* **1957**, *10*, 504. (c) Brock C. P.; Dunitz, J. D. *Acta Crystallogr., Sect. B* **1982**, *38*, 2218. (d) Oddershede, J.; Larsen, S. *J. Phys. Chem. A* **2004**, *108*, 1057.

(15) Hazell, A. C.; Hazell, R. G.; Norskov-Lauritsen, L.; Briant, C. E.; Jones, D. W. *Acta Crystallogr., Sect.* C **1986**, *42*, 690.

(16) Balasubramaniyan, V. *Chem. Rev.* **1966**, *66*, 567.

(17) (a) Schmidbaur, H.; Öller, H.-J.; Wilkinson, D. L.; Huber B.; Müller, G. *Chem. Ber.* **1989**, *122*, 31. (b) Fujihara H.; Furukawa, N. *J. Mol. Struct.* **1989**, *186*, 261. (c) Fujihara, H.; Akaishi, R.; Erata, T.; Furukawa, N. *J. Chem. Soc., Chem. Commun.* **1989**, 1789. (d) Handal, J.; White, J. G.; Franck, R. W.; Yuh, Y. H.; Allinger, N. L. *J. Am. Chem. Soc.* **1977**, *99*, 3345. (e) Blount, J. F.; Cozzi, F.; Damewood, J. R.; Iroff, D. L.; Sjöstrand U.; Mislow, K. *J. Am. Chem. Soc.* **1980**, *102*, 99. (f) Anet, F. A. L.; Donovan, D.; Sjöstrand, U.; Cozzi F.; Mislow, K. *J. Am. Chem. Soc.* **1980**, *102*, 1748. (g) Hounshell, W. D.; Anet, F. A. L.; Cozzi, F.; Damewood Jr., J. R.; Johnson, C. A.; Sjöstrand U.; Mislow, K. *J. Am. Chem. Soc.* **1980**, *102*, 5941. (h) Schröck, R.; Angermaier, K.; Sladek, A.; Schmidbaur, H. *Organometallics* **1994**, *13*, 3399.

(18) (a) Kilian, P.; Knight, F. R.; Woollins, J. D. *Chem. Eur. J.* **2011**, *17*, 2302. (b) Kilian, P.; Knight, F. R.; Woollins, J. D. *Coord. Chem. Rev.* **2011**, *255*, 1387.

(19) (a) Meinwald, J.; Dauplaise, D.; Wudl F.; Hauser, J. J. *J. Am. Chem. Soc.* **1977**, *99*, 255. (b) Ashe III, J A. J.; Kampf, W.; Savla, P. M. *Heteroat. Chem.* **1994**, *5*, 113. (c) Lanfrey, M. *Compt. Rend.* **1911**, *152*, 92. (d) Price, W. B.; Smiles, S. *J. Chem. Soc.* **1928**, 2372. (e) Zweig, A.; Hoffman, A. K. *J. Org. Chem.* **1965**, *30*, 3997. (f) Kilian, P.; Philp, D.; Slawin, A. M. Z.; Woollins, J. D.; *Eur. J. Inorg. Chem.* **2003**, 249. (g) Wawrzyniak, P.; Fuller, A. L.; Slawin, A. M. Z.; Kilian, P. *Inorg. Chem.* **2009**, *48*, 2500.

(20) (a) Aucott, S. M.; Milton, H. L.; Robertson, S. D.; Slawin, A. M. Z.; Walker, G. D.; Woollins, J. D. *Chem. Eur. J.* **2004**, *10*, 1666. (b) Aucott, S. M.; Milton, H. L.; Robertson, S. D.; Slawin A. M. Z.; Woollins, J. D. *Heteroat. Chem.* **2004,** *15*, 530. (c) Aucott, S. M.; Milton, H. L.; Robertson, S. D.; Slawin, A. M. Z.; Woollins, J. D. *Dalton Trans.* **2004**, 3347. (d) Aucott, S. M.; Kilian, P.; Milton, H. L.; Robertson, S. D.; Slawin, A. M. Z.; Woollins, J. D. *Inorg. Chem.* **2005**, *44*, 2710. (e) Aucott, S. M.; Kilian, P.; Robertson, S. D.; Slawin, A. M. Z.; Woollins, J. D. *Chem. Eur. J.* **2006**, *12*, 895. (f) Aucott, S. M.; Duerden, D.; Li, Y.; Slawin, A. M. Z.; Woollins, J. D. *Chem. Eur. J.* **2006**, *12*, 5495.

(21) (a) Kilian, P.; Slawin, A. M. Z.; Woollins, J. D. *Dalton Trans.* **2003**, 3876. (b) Kilian, P.; Slawin, A. M. Z.; Woollins, J. D. *Chem. Eur. J.* **2003**, *9*, 215. (c) Kilian, P.; Slawin, A. M. Z.; Woollins, J. D. *Chem. Commun.* **2003**, 1174. (d) Kilian, P.; Milton, H. L.; Slawin, A. M. Z.; Woollins, J. D. *Inorg. Chem.* **2004**, *43*, 2252. (e) Kilian, P.; Slawin, A. M. Z.; Woollins, J. D. *Inorg. Chim. Acta* **2005**, *358*, 1719. (f) Kilian, P.; Slawin, A. M. Z.; Woollins, J. D. *Dalton Trans.* **2006**, 2175.

(22) (a) Knight, F. R.; Fuller, A. L.; Slawin, A. M. Z.; Woollins, J. D. *Dalton Trans.* **2009**, 8476. (b) Knight, F. R.; Fuller, A. L.; Slawin, A. M. Z.; Woollins, J. D. *Polyhedron* **2010**, *29*, 1849. (c) Knight, F. R.; Fuller, A. L.; Slawin, A. M. Z.; Woollins, J. D. *Polyhedron* **2010**, *29*, 1956. (d) Knight, F. R.; Fuller, A. L.; Slawin, A. M. Z.; Woollins, J. D. *Chem. Eur. J.* **2010**, *16*, 7617.

(23) Knight, F. R.; Fuller, A. L.; Bühl, M.; Slawin, A. M. Z.; Woollins, J. D. *Chem. Eur. J.* **2010**, *16*, 7503.

(24) (a) Knight, F. R.; Fuller, A. L.; Bühl, M.; Slawin, A. M. Z.; Woollins, J. D. *Inorg. Chem.* **2010**, *49*, 7577. (b) Knight, F. R.; Fuller, A. L.; Slawin, A. M. Z.; Woollins, J. D. *Eur. J. Inorg. Chem,* **2010**, 4034.

(25) Knight, F. R.; Fuller, A. L.; Bühl, M.; Slawin, A. M. Z.; Woollins, J. D. *Chem. Eur. J.* **2010**, *16*, 7605.

(26) (a) Fuller, A. L.; Knight, F. R.; Slawin, A. M. Z.; Woollins, J. D. *Acta Crystallogr., Sect. E* **2007**, *E63*, o3855. (b) Fuller, A. L.; Knight, F. R.; Slawin, A. M. Z.; Woollins, J. D. *Acta Crystallogr., Sect. E* **2007**, *E63*, o3957. (c) Fuller, A. L.; Knight, F. R.; Slawin, A. M. Z.; Woollins, J. D. *Acta Crystallogr., Sect. E* **2008**, *E64*, o977.

(27) Aschenbach, L. K.; Knight, F. R.; Randall, R. A. M.; Cordes, D. B.; Baggott, A.; Bühl, M.; Slawin, A. M. Z.; Woollins, J. D. *Dalton Trans.* **2012**, *41*, 3141.

(28) Knight, F. R.; Athukorala Arachchige, K. S.; Randall, R. A. M.; Bühl, M.; Slawin, A. M. Z.; Woollins, J. D. *Dalton Trans.* **2012**, *41*, 3154.

(29) Nagy, P.; Szabó, D.; Kapovits, I.; Kucsman, Á.; Argay, G.; Kálmán, A. *J. Mol. Struct.* **2002**, *606*, 61.

(30) Fujihara, H.; Ishitani, H.; Takaguchi, Y.; Furukawa, N. *Chem. Lett.* **1995**, 7, 571.

(31) Balzer, G.; Duddeck, H.; Fleischer, U.; Röhr, F. *Fresenius' J. Anal. Chem.* **1997**, *357*, 473.

(32) Griffin, J. M.; Knight, F. R.; Hua, G.; Ferrara, J. S.; Hogan, S. W. L.; Woollins, J. D.; Ashbrook, S. E. *J. Phys. Chem.* C **2011**, *115*, 10859.

(33) (a) Nishio, M. *CrystEngComm.* **2004**, *6*, 130. (b) Fischer, C.; Gruber, T.; Seichter, W.; Schindler, D.; Weber, E. *Acta Crystallogr. Sec. E* **2008**, *E64*, o673. (c) Hirota, M.; Sakaibara, K.; Suezawa, H.; Yuzuri, T.; Ankai, E.; Nishio, M. *J. Phys. Org. Chem.* **2000**, *13*, 620. (d) Tsubaki, H.; Tohyama, S.; Koike, K.; Saitoh, H.; Ishitani, O. *Dalton Trans.* **2005**, 385.

(34) (a) Spek, A. L. *J. Appl. Cryst.* **2003**, *36*, 7. (b) Spek, A. L. *Acta Crystallogr., Sect. D* **2009,** *65*, 148.

(35) Bondi, A. *J. Phys. Chem.* **1964**, *68*, 441.

(36) (a) Roesky, H.W.; Andruh, M. *Coord. Chem. Rev.* **2003**, *236*, 91. (b) Koizumi, T.; Tsutsui, K.; Tanaka, K. *Eur. J. Org. Chem.* **2003**, 4528. (c) Janiak, C. *J. Chem. Soc., Dalton Trans.* **2000**, 3885.

(37) E.g. the parent 1,8-bis(dimethylphosphine)naphthalene: Jones, P. G.; Thonnessen, H.; Karacar, A.; Schmutzler, R. *Acta Crystallogr., Sect.* C **1997**, *53*, 1119.

(38) Wiberg, K. B. *Tetrahedron* **1968**, *24*, 1083.

(39) Reed, A. E.; Curtiss, F.; Weinhold, L. A. F. *Chem. Rev.* **1988**, *88*, 899.

BRIEFS (WORD Style "BH_Briefs"). If you are submitting your paper to a journal that requires a brief, provide a one-sentence synopsis for inclusion in the Table of Contents.

SYNOPSIS TOC (Word Style "SN_Synopsis_TOC"). If you are submitting your paper to a journal that requires a synopsis graphic and/or synopsis paragraph, see the Instructions for Authors on the journal's homepage for a description of what needs to be provided and for the size requirements of the artwork.

JACS Authors note: Authors are required to submit a graphic entry for the Table of Contents (TOC) that, in conjunction with the manuscript title, should give the reader a representative idea of one of the following: A key structure, reaction, equation, concept, or theorem, etc., that is discussed in the manuscript. The TOC graphic may be ***no wider than 9.0 cm*** and ***no taller than 3.5 cm*** as the graphic will be reproduced at 100% of the submission size. A surrounding margin will be added to this width and height during *Journal* production.